Fisher, A. B., Furia, L., & Berman, H. (1980) *J. Appl. Physiol.: Respir., Environ. Exercise Physiol. 49*, 743–750.
Fulmer, J., Elson, N., Bradley, K., Ferrans, V., & Crystal, R. (1977) *Clin. Res. 25*, 416A.
Jaffe, E. A., Leung, L. L. K., Nachman, R. L., Levin, R. I., & Mosher, D. F. (1982) *Nature (London) 295*, 246–248.
Kawanami, O., Ferrans, V. J., & Crystal, R. G. (1982) *Lab. Invest. 46*, 39–53.
Kniazeff, A. J., Stoner, G. D., Terry, L., Wagner, R. M., & Hoppenstand, R. D. (1976) *Lab. Invest. 34*, 495–500.
Kuhn, C., III (1976) *Lung Biol. Health Dis. 2*, 49–71.
Lowry, O. H., Rosenbrough, N. J., Farr, A. L., & Randall, R. J. (1951) *J. Biol. Chem. 193*, 265–275.
Madri, J. A., & Furthmayr, H. (1980) *Hum. Pathol. 11*, 353–366.
McPherson, J., Sage, H., & Bornstein, P. (1981) *J. Biol. Chem. 256*, 11330–11336.
Mosher, D. F., Doyle, M. J., & Jaffe, E. A. (1982) *J. Cell Biol. 93*, 343–348.
Raugi, G. J., Mumby, S. M., Abbott-Brown, D., & Bornstein, P. (1982) *J. Cell Biol. 95*, 351–354.
Rennard, S. I., & Crystal, R. G. (1982) *J. Clin. Invest. 69*, 113–122.
Sage, H. (1983) in *The Biology of the Endothelial Cell* (Jaffe, E. A., Ed.) Nijhoff, The Netherlands (in press).
Sage, H., & Bornstein, P. (1982) *Methods Enzymol. 82*, 96–127.
Sage, H., Crouch, E., & Bornstein, P. (1979) *Biochemistry 18*, 5433–5442.
Sage, H., Pritzl, P., & Bornstein, P. (1981) *Arteriosclerosis (Dallas) 1*, 427–442.
Saglio, S. D., & Slayter, H. S. (1982) *Blood 59*, 162–166.
Sahu, S. C., Tanswell, A. K., & Lynn, W. S. (1980) *Lung 158*, 143–150.
Tanswell, A. K., & Smith, B. T. (1980) *Birth Defects, Orig. Artic. Ser. 16*, 249–259.
Villiger, B., Kelley, D. G., Engleman, W., Kuhn, C., & McDonald, J. A. (1981) *J. Cell Biol. 90*, 711–720.

Conformational Effects of Volatile Anesthetics on the Membrane-Bound Acetylcholine Receptor Protein: Facilitation of the Agonist-Induced Affinity Conversion†

Anthony P. Young‡ and David S. Sigman*

ABSTRACT: The rate of the carbamylcholine-induced affinity conversion of the membrane-bound acetylcholine receptor protein from *Torpedo californica* is enhanced by pretreatment of the membranes under an atmosphere of 3% halothane or 1% chloroform. The enhancement is much more pronounced in the presence of low rather than high concentrations of carbamylcholine since the volatile anesthetics alter the apparent dissociation constant for carbamylcholine from 17 to 3 μM without affecting the first-order rate constant for the ligand-induced conversion (0.07 s^{-1}). These results indicate that the acetylcholine receptor is assuming a conformational form with intermediate affinity for carbamylcholine in addition to the previously described low- and high-affinity forms. The dissociation constants for carbamylcholine obtained from kinetic studies of the carbamylcholine-induced transition are 3–15-fold lower than those obtained as inhibition constants from the rate of ^{125}I-labeled α-bungarotoxin binding to the low-affinity conformer of the acetylcholine receptor protein. This pattern, observed in both the presence and absence of anesthetic, provides further evidence that the acetylcholine receptor has nonequivalent ligand binding sites for carbamylcholine.

It is generally accepted that structural transitions of the acetylcholine receptor protein (AcChR) mediate the rapid agonist-induced increase in cation permeability of nicotinic postsynaptic membranes and the slower loss of permeability (desensitization) which occurs upon prolonged exposure to agonists. *Torpedo* electroplaques provide an enriched source of the AcChR, and membrane fractions prepared from this source have been used extensively to investigate the conformational properties of the AcChR (Heidmann & Changeaux, 1978; Conti-Tronconi & Raftery, 1982). Studies of agonist inhibition of the rate of radiolabeled snake α-neurotoxin binding to the AcChR (Weber et al., 1975; Weiland et al., 1976; Lee et al., 1977) as well as direct binding studies using radiolabeled (Boyd & Cohen, 1980) or fluorescent agonists (Heidmann & Changeaux, 1979a) have established that the membrane-bound AcChR from *Torpedo* undergoes a slow (seconds to minutes time scale) agonist-induced structural transition from a weak-binding to tight-binding conformer. It is likely that this structural transition is the in vitro correlate of the densensitization of receptors of postsynaptic membranes (Weber et al., 1975; Lee et al., 1977; Sine & Taylor, 1979).

Scheme I

The two-state cyclic model shown as Scheme I has been used to characterize the slow affinity conversion observed in vitro (Boyd & Cohen, 1980; Heidmann & Changeaux, 1979a; Quast et al., 1978; Weiland et al., 1977) and desensitization observed by electrophysiological procedures in situ (Katz & Thesleff, 1957; Rang & Ritter, 1970). In this scheme, R and D signify the conformers of low and high affinity of the

† From the Molecular Biology Institute and the Department of Biological Chemistry, School of Medicine, University of California, Los Angeles, California 90024. *Received October 7, 1982.* The research was supported by U.S. Public Health Service Grant 21199.
‡ Present address: Department of Pharmacology, Stanford University School of Medicine, Stanford, CA.

0006-2960/83/0422-2155$01.50/0

AcChR, respectively, K_{RL} and K_{DL} are dissociation constants which characterize the binding of agonist L to these low- and high-affinity states, respectively, and k_1, k_{-1}, k_2, and k_{-2} are rate constants which describe the reversible structural transitions.

Although Scheme I provides a satisfactory representation of the affinity conversion in vitro [Boyd & Cohen, 1980; Heidmann & Changeux, 1979a; Weiland et al., 1977; see Quast et al. (1978)], rapid agonist-induced changes in affinity of the AcChR, perhaps related to receptor activation, are still possible. If rapid isomerizations were occurring, K_{RL} would become an apparent dissociation constant which characterized agonist binding to several conformations of the AcChR (Barrantes, 1978). It follows that agents which alter the kinetics of rapid agonist-induced conformational changes should also alter K_{RL} of Scheme I.

The volatile anesthetics chloroform and halothane under certain conditions increase the time constant of decay of miniature end-plate currents (mepcs) at the neuromuscular junction (Gage & Hamil, 1976) and are therefore likely candidates to alter K_{RL} (Scheme I). We have previously shown that these agents increase the proportion of D-state AcChR present in the absence of agonist via an allosteric mechanism (Young & Sigman, 1981) and alter the kinetics of toxin binding at high concentrations (Young et al., 1981). In this paper, we analyze the effects of halothane and chloroform on the kinetics of the carbamylcholine (carb)-induced affinity conversion of the membrane-bound AcChR from *Torpedo* in terms of Scheme I. Alterations in the kinetics of ^{125}I-labeled α-bungarotoxin ([^{125}I]α-Bgt) in the presence of carb have provided the probe for AcChR conformation. The primary effect of pretreatment of membranes under an atmosphere of 3% halothane or 1% chloroform is to diminish K_{RL} from 17 to 2.7 and 3.1 μM, respectively. This perturbation by the volatile anesthetics suggests that rapid agonist-induced affinity alterations of the AcChR do indeed occur.

The dissociation constants which characterize the carb-induced transition are 3–15-fold lower than inhibition constants obtained from studies of the rate of [^{125}I]α-Bgt binding to the low-affinity conformer of the AcChR. The differences suggest that each R-state AcChR contains multiple binding sites which differ in their affinity for carb, a conclusion consistent with affinity labeling studies (Damle & Karlin, 1978; Wolosin et al., 1980), the observed multiple binding sites of the potent AcChR antagonist *d*-tubocurarine (Neubig & Cohen, 1979) and the heterogeneity in toxin binding sites created by high concentrations of volatile anesthetics and aliphatic alcohols (Young et al., 1981).

Materials and Methods

Materials

The following materials were obtained commercially: carbamylcholine chloride (carb), phenylmethanesulfonyl fluoride (PMSF), Triton X-100, and 1× recrystallized bovine serum albumin (BSA) (Sigma); lactoperoxidase (EC 1.11.1.7) (Calbiochem); Na^{125}I (New England Nuclear or Amersham); DEAE filter disks (Whatman); halothane, containing 0.01% thymol (Halocarbon Laboratories, Hackensack, NJ); analytical grade chloroform (Mallinckrodt); *Bungarus multicinctus* lyophilized venom (Miami Serpentarium, Miami, FL). All buffer components were reagent grade or better.

Methods

Purification of α-Bgt and its radioiodination to form [^{125}I]α-Bgt have been previously described (Young & Sigman, 1981). *Torpedo californica* were obtained live from Pacific Biomarine (Venice, CA). The electric organs were excised, quick frozen in liquid nitrogen, and stored at −60 °C. Membranes were prepared from electric organ pieces (50 g) (Reed et al., 1975). All measurements discussed below were made within 2–3 days of preparation of membrane fragments derived from electric organs frozen no longer than 3 months. Membranes derived from two different fish were used for measurements involving incubation under 3% halothane or 1% chloroform. Parallel control measurements were made with these membranes (controls 1 and 2, respectively). Delivery of the volatile anesthetics has been described previously (Young & Sigman, 1981).

Kinetic Procedures. For kinetic runs, membranes were pretreated for 30 min in a closed vial, under an atmosphere of medicinal-grade air, or under an atmosphere of 3% halothane or 1% chloroform. Medicinal-grade air had no effect on any parameter investigated; volatile anesthetic effects were stable between 10 and 60 min of incubation, and these effects could be reversed by passage of air over anesthetic-treated samples for 30 min. All measurements were made at 21 °C by using a thermostated water bath with solutions buffered in 0.01 M *N*-(2-hydroxyethyl)piperazine-*N*′-2-ethanesulfonic acid (Hepes), pH 7.4, 0.1 M NaCl, 1 mM ethylene glycol bis(β-aminoethyl ether)-*N*,*N*,*N*′,*N*′-tetraacetic acid (EGTA), and 3 mM NaN_3.

Membranes were pretreated with or without carb followed by addition to [^{125}I]α-Bgt (with or without carb) and assayed for either initial rates or the entire time course of toxin binding. In either case, aliquots were withdrawn and added into a solution containing 1 mg/mL α-Bgt (approximate 30-fold molar excess) and 0.1 N carb to quench the reaction followed by measuring the AcChR-bound toxin by using the DEAE filter disk assay developed by Schmidt & Raftery (1973). [^{125}I]α-Bgt was always present in 7–10-fold molar excess relative to binding sites on the membranes so that pseudo-first-order conditions (with respect to toxin) were maintained for the bimolecular association of toxin to receptor (eq 1).

$$A + T \xrightarrow{k_0} A\text{–}T \tag{1}$$

The pseudo-first-order rate constant for toxin binding, k_{app} (k_0T), was calculated by using either eq 2 or 3, depending on

$$1 - \frac{A_0 - AT}{A_0} = k_{app}t \tag{2}$$

$$\ln \frac{A_0 - AT}{A_0} = -k_{app}t \tag{3}$$

the appropriateness of the initial velocity assumption. For both of these expressions, A_0 is the total toxin binding normality of the membranes, and AT is the toxin bound at time t.

The inhibition of toxin binding by carb permitted the calculation of a dissociation constant for this agonist (K_I) since

$$\frac{d(AT)}{dt} = k_0TR = k_0T\bar{R}\frac{K_I}{L + K_I} \tag{4a}$$

$$\frac{d(AT)}{dt} = k_{app}{}^0\frac{\bar{R}K_I}{L + K_I} = k_{app}\bar{R} \tag{4b}$$

where $\bar{R} = R + RL$ and $k_{app}{}^0$ is the pseudo-first-order rate constant for toxin binding in the absence of carb (k_0T); k_{app} is the pseudo-first-order rate constant in the presence of a concentration, L, of carb [$k_{app}{}^0[K_I/(L + K_I)]$].

Kinetics of the carb-Induced Transition between Conformers of Low and High Affinity. The observed first-order rate constant for the carb-induced affinity conversion, k_i, was monitored by two procedures. The first procedure involved

Table I: Values of k_i at High Agonist Concentrations

[carb] (μM)	k_i (mean) (s^{-1})	standard deviation
	With 3% Halothane	
20	5.3×10^{-2}	$\pm 0.28 \times 10^{-2}$
30	8.1×10^{-2}	$\pm 0.71 \times 10^{-2}$
40	7.2×10^{-2}	$\pm 0.43 \times 10^{-2}$
	Control	
50	5.7×10^{-2}	$\pm 0.42 \times 10^{-2}$
75	6.0×10^{-2}	$\pm 0.70 \times 10^{-2}$

pretreatment of membranes with carb for time τ followed by assay for the initial rate of toxin binding (Weber et al., 1975; Weiland et al., 1976; Lee et al., 1977; Quast et al., 1978). The rate constant k_i is given by eq 5 where $k_{app,\tau}$ is the pseudo-

$$\ln (k_{app,\tau} - k_{app,eq}) = -k_i t \quad (5)$$

first-order rate of toxin binding obtained after time τ of pretreatment with carb and $k_{app,eq}$ is that rate observed at equilibrium after 30 min of incubation with the ligand. In all cases, k_i was obtained by exponential least-squares analysis of k_{app}'s obtained at five to eight different τ's and exhibited an average error of $\pm 13\%$.

The second procedure was employed under conditions where k_i was too large ($k_i > 0.04\ s^{-1}$) to be quantitated by the previous procedure. It involves adding membranes to carb and [^{125}I]α-Bgt simultaneously and monitoring the entire time couse of toxin binding. The loss of the R state of AcChR either by its conversion to the D state or by its binding of the toxin can be treated as a parallel first-order reaction (Frost & Pearson, 1961; Quast et al., 1978; Young, 1979). According to the two-state model, the loss of R receptor due to isomerization is described by (Janin, 1973)

$$-\frac{d\bar{R}}{dt}(\text{isomerization}) = \left[\frac{k_1 + k_2(L/K_{RL})}{1 + L/K_{RL}}\right]\bar{R} - \left[\frac{k_{-1} + k_{-2}(L/K_{DL})}{1 + L/K_{DL}}\right](A_0 - \bar{R}) \quad (6)$$

at high concentrations of carb, L/K_{DL} is large, and eq 6 reduces to

$$-\frac{d\bar{R}}{dt}(\text{isomerization}) = \left[\frac{k_1 + k_2(L/K_{RL})}{1 + L/K_{RL}}\right]\bar{R} - k_{-2}(A_0 - \bar{R}) \quad (7a)$$

Moreover, at high carb concentrations where k_i is rapid, k_{-2} contributes little to the overall isomerization rate (see Table I) so that eq 7b is valid.

$$-\frac{d\bar{R}}{dt}(\text{isomerization}) = \left[\frac{k_1 + k_2(L/K_{RL})}{1 + L/K_{RL}}\right]\bar{R} = k_i\bar{R} \quad (7b)$$

The loss of $\bar{R}$ due to toxin binding, provided in eq 4, permits the overall loss of $\bar{R}$ to be represented

$$\frac{d\bar{R}}{dt}(\text{overall}) = \frac{d\bar{R}}{dt}(\text{isomerization}) + \frac{d\bar{R}}{dt}(\text{toxin binding}) = (k_i + k_{app})\bar{R} \quad (8)$$

The fraction (f) of total receptor (A_0) present as $\bar{R}$ ($\bar{R}_0$) can be determined from the ability of 1 μM carb to inhibit toxin binding (Young & Sigman, 1981). Integration of eq 8 provides eq 9 which substituted back into eq 4b provides eq 10 after integration.

$$\bar{R} = fA_0 e^{-(k_i + k_{app})t} \quad (9)$$

$$AT = \frac{k_{app} f(A_0)}{k_i + k_{app}}[1 - e^{-(k_i + k_{app})t}] \quad (10)$$

Since the D form of the receptor binds the toxin much more slowly because of its higher affinity to L, the end point for toxin binding, AT_∞ can be derived from eq 10 to be

$$AT_\infty = \frac{k_{app} f(A_0)}{k_i + k_{app}} \quad (11)$$

Subtraction of eq 11 from eq 10 followed by algebraic rearrangement yields

$$\frac{A_0 - AT}{A_0} - \left(1 - \frac{AT_\infty}{A_0}\right) = \frac{k_{app} f}{k_i + k_{app}} e^{-(k_i + k_{app})t} \quad (12)$$

Plots of eq 12 provide $k_i + k_{app}$. Substitution of the quantity back into eq 11 yields k_{app} since AT_∞ and f are known. Then k_i can be readily determined.

The correlation coefficients for a least-squares fit to the exponential curve of eq 12 were always greater than 0.900 and frequently greater than 0.950. For example, the correlation coefficient for the plot of eq 12 in Figure 1 obtained at 5 μM carb in the absence of anesthetic yielded a value of $k_i + k_{app}$ of $7.32 \times 10^{-2}\ s^{-1}$ and a correlation coefficient of 0.994. Three tests for the accuracy and reproducibility of the values of k_i were carried out in addition to calculation of the correlation coefficients. To eliminate systematic error by the method of parallel reactions, we determined values of k_i in the concentration ranges of carb which were suitable for both methods of measurement. The data summarized in Figure 1 show that at 5 μM carb in the absence of anesthetic, the k_i measured by preincubation with the agonist was $1.9 \times 10^{-2}\ s^{-1}$ while that obtained by using the method of parallel reactions was $1.6 \times 10^{-2}\ s^{-1}$.

The second test for the accuracy of the rate constants measured by the parallel reaction technique involved evaluation of k_i at identical concentrations of agonist (1 μM carb) and halothane (3%) but at different concentrations of toxin (7.1×10^{-7} and 5.35×10^{-7} M). The quantity $k_i + k_{app}$ for the high and low toxin concentrations was 8.01×10^{-2} and $7.41 \times 10^{-2}\ s^{-1}$, respectively. Values of k_{app} determined from these slopes (eq 11) were 2.83×10^{-2} and $3.42 \times 10^{-2}\ s^{-1}$. At the relatively low agonist concentrations used in these experiments, k_{app} is approximately the product of k_0, the second-order rate constant for toxin binding, and toxin concentration. A test of the kinetics analysis is the consistency of the values calculated for k_0 at these two toxin concentrations. They are 6.9×10^4 and $6.4 \times 10^4\ M^{-1}\ s^{-1}$ at the high and low toxin concentrations, respectively. The values of k_i determined from these data are 3.20×10^{-2} and $3.99 \times 10^{-2}\ s^{-1}$. The same rate constant determined by preincubating the receptor with the agonist is $3.60 \times 10^{-2}\ s^{-1}$ (Figure 2). These results indicate a probable error for the rate constants of $\pm 25\%$.

The third test of the accuracy of our data was repetitive measurements of k_i at higher ligand concentrations. The data summarized in Table I indicate the standard deviations associated with these measurements.

Results

Determination of the Isomerization Constant (k_i). The effect of halothane on the apparent first-order rate for the affinity conversion, k_i, determined by preincubation with 1 μM

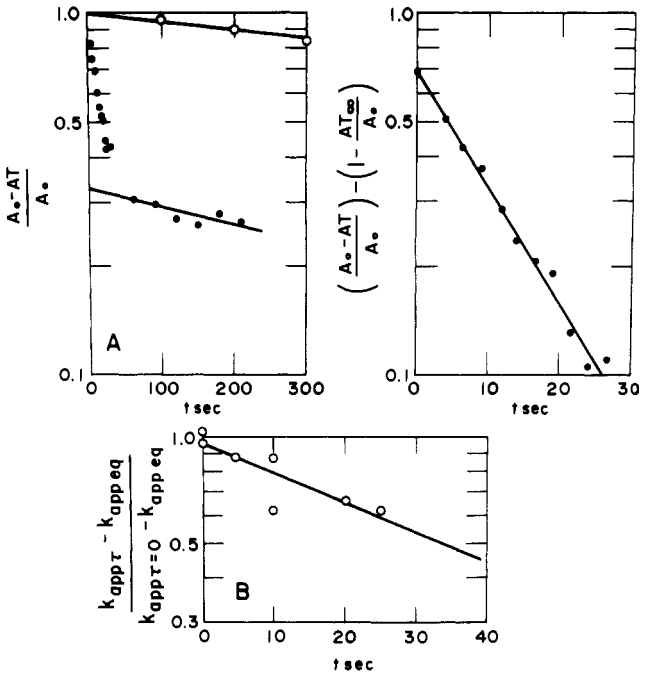

FIGURE 1: Two different procedures used to measure the rate of the affinity conversion, k_i, mediated by 5 μM carb. (A) Estimation by the method of parallel reactions (affinity conversion coincident with toxin binding). (Left panel) Membranes (control 1, 7.5×10^{-8} M in toxin binding sites) were added to 7.1×10^{-7} M [^{125}I]α-Bgt and 5 μM carb, and the time course of toxin binding was monitored (●). Also shown in the figure is the time course of toxin binding after membrane pretreatment with 5 μM carb (○). The parameter AT_∞/A_0 was determined from these data as discussed in the text (eq 11). (Right panel) The data were plotted in accordance with eq 12, yielding $k_i + k_{app}$ as 7.32×10^{-2} s^{-1}. From these data, k_i is calculated to be 1.64×10^{-2} s^{-1}. (B) Estimation based on preincubation with carb. Membranes (control 1, 4.6×10^{-8} M in toxin binding sites) were pretreated with 5 μM carb for the indicated times prior to addition to 4.3×10^{-7} M [^{125}I]α-Bgt and assay for the initial rates of toxin binding. The data are plotted in accordance with eq 5; $k_i = 1.9 \times 10^{-2}$ s^{-1}.

carb, is summarized in Figure 2. Pretreatment of membranes under an atmosphere of 3% halothane for 30 min results in a 4-fold increase in k_i. Similar results are obtained by using 1% chloroform. Since 3–10 s is required to measure the initial rates of toxin binding, values of k_i greater than 0.04 s^{-1} ($t_{1/2}$ = 17 s) are too fast to measure by this procedure. Therefore, k_i was obtained in this fashion with 0.5 μM ≥ carb ≤ 10 μM for control membranes and with 0.3 μM ≥ carb ≤ 2 μM for membranes treated with 3% halothane or 1% chloroform. These data are included in Figures 3 and 4. At higher concentrations, k_i was monitored by using the method of parallel reactions. Under Materials and Methods, evidence for the accuracy of this procedure is provided. Values of k_i measured at carb concentrations where both approaches are applicable give internally consistent results (Figure 1).

Analysis of k_i in Terms of Scheme I. The dependence of the observed rate constant k_i on carb concentration shown in Figures 3 and 4 suggests that the primary effect of anesthetics is to lower the concentration of carb where conversion will occur at its half-maximal rate. To establish this point in a quantitative fashion, we have analyzed the data with regard to the two-state cyclic model (Scheme I) where the definition of k_i in terms of this scheme is (Janin, 1973)

$$k_i = \frac{k_1 + k_2(L/K_{RL})}{1 + L/K_{RL}} + \frac{k_{-1} + k_{-2}(L/K_{DL})}{1 + L/K_{DL}} \quad (13)$$

In order to analyze the data of Figures 3 and 4 in terms of

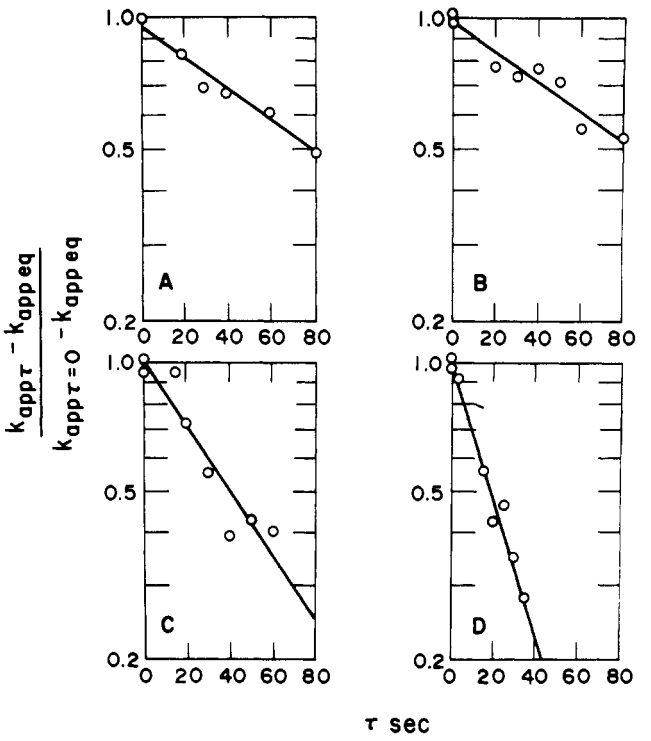

FIGURE 2: Acceleration by halothane of the rate of the affinity conversion, k_i, mediated by 1 μM carb. Rates of toxin binding (k_{app}) were determined as a function of the time of pretreatment of membranes with 1 μM carb after preequilibration of membranes under an atmosphere of 0 (A), 1% (B), 2% (C), or 3% (D) halothane. Initial rates of toxin binding are plotted in accordance with eq 4. Values of k_i are 0.850 (A), 0.791 (B), 1.79 (C), and 3.60×10^{-2} s^{-1} (D).

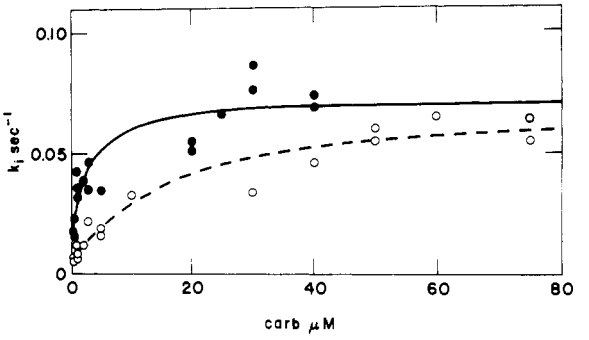

FIGURE 3: Affinity conversion as a function of carb concentration with and without membrane pretreatment with 3% halothane analyzed by the two-state model. Values for k_i, obtained as discussed in the text, are plotted as a function of carb concentration for membranes pretreated with (●) and without (○) 3% halothane. The lines drawn are based on the best fits of the data from nonlinear regression analysis as discussed in the text for the membranes treated with (—) and without (- - -) halothane. K_{DL} was assumed to be 0.045 and 0.037 μM for the membranes treated with and without halothane, respectively.

eq 13 which contains six variables, five of which are independent, we determined the values of k_{-1}, k_1, and K_{DL} in separate experiments.

Estimation of k_{-1} and k_1. The rate constants k_{-1} and k_1 are readily obtained through toxin binding studies (Quast et al., 1978). The ratio R/D is defined by Scheme I as k_{-1}/k_1 and is obtained by comparison of the initial rates of toxin binding in the presence and absence of 1 μM carb. At this concentration, carb totally inhibits toxin binding to the D-state AcChR while binding of toxin to the R-state AcChR is uninhibited (Quast et al., 1978; Young & Sigman, 1981). For control 1, control 2, 3% halothane, and 1% chloroform membranes, k_{-1}/k_1 is 7.3, 8.6, 3.3, and 3.9, respectively.

Table II: Rate and Equilibrium Constants of Scheme I

	K_{DL} (μM)[a]	k_{-1} (s^{-1})[b]	k_1 (s^{-1})[b]	k_{-2} (s^{-1})[c]	k_2 (μM)[d]	K_{RL}, (μM)[d]	K_{ov}(calcd)[e] (μM)	K_{ov}(exptl)[f] (μM)
control 1	0.037[g]	1.6×10^{-2}	2.2×10^{-3}	1.1×10^{-3}	7.1×10^{-2}	17.2	0.30	0.14 ± 0.03
	0.043[h]	1.6×10^{-2}	2.2×10^{-3}	1.2×10^{-3}	7.2×10^{-2}	18.0	0.34	
3% halothane	0.045[g]	2.2×10^{-2}	6.6×10^{-3}	3.8×10^{-3}	6.9×10^{-2}	2.7	0.18	0.11 ± 0.02
	0.058[h]	2.2×10^{-2}	6.6×10^{-3}	4.6×10^{-3}	6.9×10^{-2}	2.9	0.24	
control 2	0.024[g]	9.5×10^{-3}	1.1×10^{-3}	9.4×10^{-4}	7.9×10^{-2}	17.4	0.23	0.16 ± 0.01
1% chloroform	0.036[g]	1.1×10^{-2}	2.8×10^{-3}	3.1×10^{-3}	6.9×10^{-2}	3.1	0.17	0.091 ± 0.004

[a] Determined independently of the data on the rate for the affinity conversion as discussed in the text. For control 1 and 3% halothane-treated membranes, K_{DL} was obtained in two slightly different fashions. Kinetic analysis was conducted by using each value for K_{DL} in these cases. [b] Determined independently of the data on the rate for the affinity conversion as discussed in the text. [c] Determined from a thermodynamic constraint on the two-state scheme $k_{-2} = k_2(K_{DL}/K_{RL})(k_{-1}/k_1)$. [d] Determined by nonlinear regression analysis of the data on the rate for the affinity conversion by using the independent determinations of k_{-1}, k_1, and K_{DL} as discussed in the text. [e] Determined by use of eq 15 and the values for K_{RL}, K_{DL}, and k_{-2} shown in this table. [f] K_{ov} determined experimentally from toxin binding data by use of eq 3. The values of K_{ov} are shown as mean values on the basis of four determinations at carb concentrations varied between 0.3 and 0.6 μM. [g] Determined with partially converted AcChR. [h] Determined with fully converted AcChR.

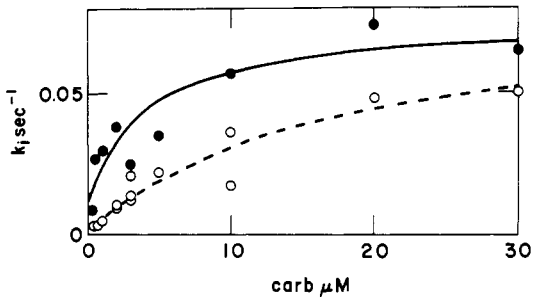

FIGURE 4: Affinity conversion as a function of carb concentration with and without membrane pretreatment with 1% chloroform analyzed by the two-state model. Values for k_i, obtained as discussed in the text, are plotted as a function of carb concentration for membranes pretreated with (●) and without (○) 1% chloroform. The lines drawn are based on the best fits of the data from nonlinear regression analysis as discussed in the text for the membranes treated with (—) and without (- - -) chloroform.

Membrane-bound AcChR incubated with carb followed by dilution converts from the D state to the R state. The observed first-order rate constant of recovery of R-state AcChR is defined by Scheme I as $k_{-1} + k_1$. This rate can be determined in a fashion analogous to that for k_i by procedure 1. Membranes were pretreated with 1.75 or 3 μM carb followed by 100- or 200-fold dilution for time t and then added to 1 μM carb and [^{125}I]α-Bgt with the initial rate of toxin binding assayed. The rates of recovery are obtained from semilog plots based on eq 14 as shown in Figure 5. From these rates and

$$\ln (k_{app,\infty} - k_{app,\tau}) = -(k_1 + k_{-1})t \qquad (14)$$

the data for k_{-1}/k_1 shown above, the values for k_{-1} and k_1 shown in Table II were obtained.

Estimation of K_{DL}. Since carb is a competitive inhibitor of toxin binding (Quast et al., 1978; Young & Sigman, 1981), K_{DL} can be obtained from the inhibition by carb of [^{125}I]α-Bgt binding to the D-state AcChR. Two methods were used to measure the inhibition constant K_{DL}. In the first, initial rates of toxin binding were estimated immediately after the AcChR was converted completely to the D state by pretreatment with 1.26–3.78 μM carb followed by 12.6-fold dilution (Quast et al., 1978). In the second method, AcChR was incubated with submicromolar concentrations of carb followed by assay of the entire time course of toxin binding. Under these conditions, AcChR is converted only partially to the D state, and inhibition constants were calculated from the slow phase of toxin binding. The values for K_{DL} shown in Table II are in good agreement with those described by other workers using direct binding (Boyd & Cohen, 1980) or toxin inhibition kinetics (Quast et al., 1978; Weiland et al., 1977).

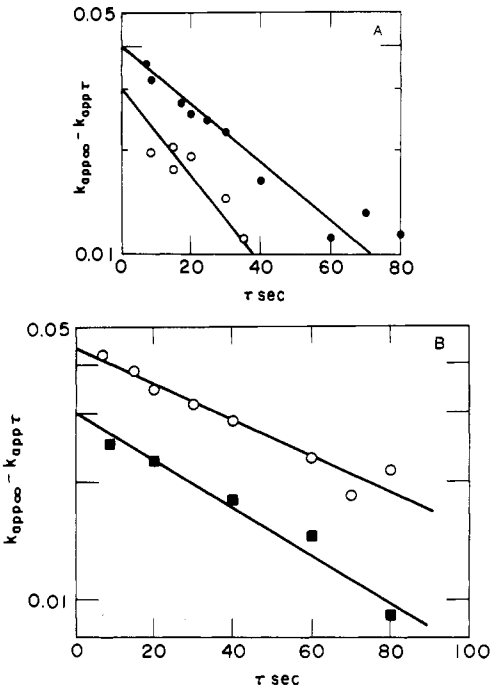

FIGURE 5: (A) Kinetics of conversion from the high-affinity state to the low-affinity state in the presence and absence of 3% halothane. Membranes (specimen 1, 3.4 μM toxin binding sites) were pretreated for 30 min with 3 μM carb, diluted 200-fold for time τ prior to addition to 2.1×10^{-7} [^{125}I]α-Bgt and 1 μM carb, and assayed for the initial rate of toxin binding. The data are plotted in accordance with eq 14 for membranes pretreated with (○) and without (●) 3% halothane. Least-squares analysis gives $k_{-1} + k_1$ equal to 2.86×10^{-2} and 1.83×10^{-2} s^{-1} for 3% halothane-treated and control membranes, respectively. (B) Kinetics of conversion from the high-affinity state to the low-affinity state in the presence and absence of 1% chloroform. Membranes (specimen 2, 3.2 μM in toxin binding sites) were pretreated for 30 min with 1.75 μM carb, diluted 100-fold for time τ prior to addition to 3.1×10^{-7} M [^{125}I]α-Bgt and 1 μM carb, and assayed for the initial rate of toxin binding. The data are plotted in accordance with eq 13 for membranes pretreated with (■) and without (○) 1% chloroform. Least-squares analysis gives $k_{-1} + k_1$ equal to 1.38×10^{-2} and 1.06×10^{-2} s^{-1} in the presence and absence of 1% chloroform, respectively.

Estimation of K_{RL} and k_2 by Nonlinear Regression Analysis. The values of K_{RL} and k_2 shown in Table II were determined by fitting the data shown in Figures 3 and 4 to eq 13 by nonlinear regression analysis using independently determined values of k_{-1}, k_1, and K_{DL} and the additional constraint that

$$k_{-2} = k_2\left(\frac{K_{DL}}{K_{RL}}\right)\left(\frac{k_{-1}}{k_1}\right) \qquad (15)$$

A useful test of the validity of the various constants was to calculate the equilibrium constant K_{ov} (eq 16). This constant

$$K_{ov} = \frac{(R + D)L}{RL + DL} = \frac{K_{RL}(k_{-2}/k_2) + K_{DL}}{1 + k_{-2}/k_2} \quad (16)$$

can be experimentally determined by incubating membranes in the low-affinity form with low concentrations of carb (e.g., 0.3 μM) and measuring the inhibition of toxin binding. The calculated values for K_{ov} are within a factor of 2 of the experimentally determined constants (Table II).

Useful conclusions can be deduced from the data reported as parameters of Scheme I which remain valid even if this scheme represents an oversimplification of the reaction mechanism. The major effect of 3% halothane or 1% chloroform is to decrease by 6.4-fold or 5.6-fold, respectively, the concentration of carb (i.e., K_{RL}) required to generate an observed rate constant that is 50% of the maximal rate constant. The first-order rate constant constant (k_2) which describes the conversion of RL $\rightarrow$ DL is not changed substantially by anesthetics. These estimates of K_{RL} and k_2 are marginally affected even if K_{DL}, k_1, and k_{-1} are allowed to change by factors of 2–3. If the value of K_{RL} used to fit the kinetic data for the halothane-facilitated conformational transition is assumed to be identical with that obtained in the absence of anesthetic (i.e., 20 μM), the calculated value of k_i is outside our experimental error at all concentrations of carb and off by a factor of 2–3 in the high concentration range.

Other significant results from the data of Table II are that the conversion of the AcChR from the R state to the D state in the absence of agonists via an allosteric mechanism (Young & Sigman, 1981) is primarily accomplished by an increase in k_1, the rate constant for the reaction R $\rightarrow$ D, rather than a decrease in k_{-1}, the rate constant governing the isomerization D $\rightarrow$ R. This point is emphasized by the increased rate of recovery from the D state to the R state observed in the presence of halothane or chloroform (Figure 5A,B). Finally, the anesthetics have only a small effect on the direct binding of carb since K_{DL} is marginally affected by halothane or chloroform.

Since neither anesthetic affects the binding of carb to the D form, it is unlikely that the anesthetics increased the binding of carb to the R form to this extent. However, inclusion of an intermediate in the R $\rightarrow$ D conversion which binds carb tighter than R-state AcChR (see eq 17) can explain these data.

$$R + L \underset{}{\overset{K_{RL}'}{\rightleftharpoons}} RL \underset{k_b'}{\overset{k_a'}{\rightleftharpoons}} IL \xrightarrow{k_c'} DL$$

In this scheme, the formation of DL can be described in differential form by

$$\frac{d(DL)}{dt} = \frac{[k_c'k_a'/(k_a' + k_b' + k_c')]L(A_0 - DL)}{[K_{RL}'(k_b' + k_c')/(k_a' + k_b' + k_c')] + L} \quad (17)$$

If k_a' and k_b' are much greater than k_c', then this expression reduces to

$$\frac{d(DL)}{dt} = \frac{[k_a'k_c'/(k_a' + k_b')]L(A_0 - DL)}{[K_{RL}'(k_b' + k_c')/(k_a' + k_b')] + L} = \frac{k_{max}L(A_0 - DL)}{K_{app} + L}$$

where $k_{max} = k_c'[k_a'/(k_a' + k_b')]$ and $K_{app} = K_{RL}'[k_b'/(k_a' + k_b')]$.

The effects of volatile anethetics can be interpreted by assuming these agents decrease the ratio k_b'/k_a'. If k_a' is significantly greater than k_b', k_{max} approaches k_c' and will be unaffected by a decrease in k_b'/k_a'. However, K_{app} which is approximately K_{RL} (k_b'/k_a') will be decreased by a decrease in k_b'/k_a'. The differential effects of the volatile anesthetics on K_{app} can be similarly interpreted in terms of more complex schemes which include isomerizations between unliganded conformers and reversible binding of the ligand to the intermediate conformer (Young, 1979).

Nonequivalence of carb Sites. Determining the concentration at which the agonist-induced conversion is 50% of the maximal rate (i.e., K_{RL}) is one approach to assess the affinity of carb for its binding site(s) on the R form of the AcChR. The ability of carb to inhibit toxin binding to the low-affinity form is a second approach. In addition to providing the apparent first-order rate constant for the ligand-induced conformational change (k_i), the analysis using parallel first-order reaction kinetics also yields the pseudo-first-order rate constant for toxin binding to the R state of the AcChR (k_{app}). In eq 4, simple expressions have been presented which allow the calculation of the inhibition constant for toxin binding by assuming the agonist blocks all toxin sites equivalently. For control membranes containing the receptor with low affinity, the inhibition constants for carb based on toxin binding are 56 ± 8 and 81 ± 8 μM for the two different preparations used in this study. For 3% halothane- and 1% chloroform-treated membranes, the corresponding constants are 25 ± 7 and 48 ± 15 μM, respectively. These values are greater than K_{RL} by 3–5-fold in the absence of anesthetic and 8–15-fold in the presence of halothane or chloroform.

Since these differences are outside experimental error, particularly in the presence of halothane or chloroform, this divergence suggests that the carb binding sites on the low-affinity form of AcChR responsible for the affinity conversion are not those being measured by the toxin binding kinetics. Possibly toxin does not bind to the site at which carb induces the affinity conversions, but it competes with carb at an additional site on the low-affinity AcChR. If this were the case, the two dissociation constants would not be expected to be equivalent. However, this mechanism is not consistent with the accumulating chemical modification evidence for two agonist sites which both bind toxin (see Discussion).

These data can be understood in terms of a model with two carb binding sites on the low-affinity AcChR which have different affinities for the agonist yet bind toxin equivalently. If each of the two sites contributes 50% of the total toxin binding titer and the rate of toxin binding to each site is identical (Blanchard et al., 1979; Young et al., 1981), the rate of toxin binding to the two sites R_1 and R_2 can be represented as

$$\frac{d(AT)}{dt} = k_aR_1T + k_aR_2T = k_aT(R_1 + R_2) \quad (18)$$

where k_a is the bimolecular rate constant for toxin binding and T is the concentration of toxin. If $K_{(1)}$ and $K_{(2)}$ represent the dissociation constants of carb for the two sites on the low-affinity AcChR, then the rate of toxin binding can be summarized by eq 19 where A represents the toxin binding titer.

$$\frac{d(AT)}{dt} = \frac{k_aT(0.5A)}{1 + L/K_{(1)}} + \frac{k_aT(0.5A)}{1 + L/K_{(2)}} = k_aTA\left[\frac{0.5}{1 + L/K_{(1)}} + \frac{0.5}{1 + L/L_{(2)}}\right] \quad (19)$$

The net result is that the application of eq 4 for the calculation of the inhibition constant provides a weighted average of carb's affinity for the two toxin binding sites. Since the experiments are complex, sufficient data have not been gathered at a variety

of carb concentrations to permit an accurate determination of the dissociation constant of the site with lowest affinity. Approximate calculations suggests that the value is approximately 200 ± 100 μM. Halothane (3%) has no apparent effect on this constant within experimental uncertainty.

Discussion

Two major conclusions have been derived from the data contained in this paper. First, the apparent dissociation constant for carb (K_{RL}) with the R-state AcChR, obtained through studies on the kinetics of the carb-induced affinity conversion, is lowered by the volatile anesthetics halothane and chloroform. This perturbation suggests rapid isomerizations of the AcChR, accompanied by alterations in affinity for agonists, prior to the slow agonist-induced conversion to the high-affinty conformation. Second, the inhibition of toxin binding to the low-affinity AcChR by carb is characterized by an inhibition constant which is severalfold higher than the apparent dissociation constant derived from the studies on the carb-induced conversion. This difference indicates two carb binding sites on the AcChR which have different affinities for carb when the protein is in its resting conformation(s) with low affinity for agonists.

Evidence for two distinct ligand binding sites on the AcChR is substantial. Both of the two toxin binding sites on the AcChR can be labeled with *p*-(trimethylammonium)-benzenediazonium fluoroborate (Weiland et al., 1979). However, after reduction with dithiothreitol, only one toxin binding site is affinity labeled with [4-(*N*-maleimido)-benzyl]trimethylammonium iodide (MBTA) (Damle & Karlin, 1978). Recent data indicate that both toxin binding sites on the reduced AcChR can be alkylated with bromoacetylcholine. However, labeling at one site requires higher concentrations of the agonist than labeling at the other (Wolosin et al., 1980). Additional evidence for the nonequivalence of the sites is that the cholinergic antagonist, *d*-tubocurarine, binds to different sites on the AcChR with vastly different affinities (K_d = 33 nM and 8 μM) (Neubig & Cohen, 1979), and rapid kinetic studies using ethidium bromide as a fluorescent probe have indicated multiple binding sites for carb (Quast et al., 1979). In the presence of high concentrations of volatile anesthetics or aliphatic alcohols, two classes of toxin binding sites differing by as much as 20-fold in their association rate constant for α-Bgt are observed (Young et al., 1981).

Our data indicate that the R form of the AcChR contains at least two binding sites with different affinities for carb, but binding at one site is sufficient to cause conversion to the high-affinity state. The diminution in $K_{(1)}$ (i.e., K_{RL}) caused by the volatile anesthetics is interpreted by assuming that these agents stabilize a transitory intermediate in the conversion pathway. It is tempting to conclude that this intermediate corresponds to the activated AcChR. However, this interpretation ignores the possible contribution of carb binding to the lowest affinity site [defined by $K_{(2)}$] in the process of receptor activation. Electrophysiological evidence (Stevens, 1976), as well as recent ion flux studies using *Torpedo* electroplaques (Neubig & Cohen, 1980), indicates that at least two agonists are required to activate the AcChR. Furthermore, the concentrations of carb required to facilitate ion flux are in the millimolar range (Neubig & Cohen, 1980), a concentration in excess of our reported values of K_{RL} (Table II). Our studies support the notion that volatile anesthetics stabilize a conformation of the AcChR with intermediate affinity for agonists. It should be emphasized, however, that it has not been determined whether this conformational state allows ion flux. We have previously reported that anesthetics stabilize the D state of the AcChR (at slightly higher concentrations than those used here) via an allosteric mechanism. This effect might be important in the inhibition of synaptic transmission by these agents (Young & Sigman, 1981). If the conformation of the AcChR with intermediate affinity for agonists is nonconducting as well, the stabilization of this conformer by the volatile anesthetics chloroform and halothane would also be important to the pharmacological effects of these compounds.

The volatile anesthetics chloroform and halothane produce structural perturbations of the membrane-bound AcChR similar to those produced by local anesthetics. Both local (Heidmann & Changeux, 1979b) and volatile anesthetics (Young & Sigman, 1981) act as allosteric effectors of the AcChR and cause conversion to the high-affinity state in the absence of agonist. Local and volatile anesthetics also have similar effects on the agonist-induced conversion. Local anesthetics increase the apparent first-order rate constant for the agonist-induced conversion, but this effect is more substantial in the presence of low rather than high concentrations of agonist. Moreover, the bimolecular rate constant for the association of 6-[5-(dimethylamino)-1-naphthalenesulfonamido]hexanoic acid β-methobromide) ethyl ester, a fluorescent agonist, to the low-affinity AcChR is increased by local anesthetics (Heidmann & Changeux, 1979b). These observations suggest that local anesthetics alter the binding of agonists to the low-affinity AcChR in a manner similar to chloroform and halothane. It has been suggested that local anesthetics produce their effects by direct binding to a modifier site which might comprise the ion channel of the AcChR (Heidmann & Changeux, 1979b). This notion is supported by the saturable binding of the radiolabeled local anesthetic meproadifen to *Torpedo* electroplaques (Krodel et al., 1979). The physical nature of the interaction between the volatile anesthetics and the AcChR is not clear. Direct binding to the protein and anesthetic-induced disruption of protein–lipid interactions are two tenable mechanisms for the action of volatile anesthetics on the membrane-bound AcChR.

Acknowledgments

We thank Janis R. Oshiki for expert experimental assistance and Dr. Julio Vargos, Department of Physiology, UCLA, for advice on the computational analysis.

Registry No. Carbamylcholine, 462-58-8; haloethane, 151-67-7; chloroform, 67-66-3.

References

Barrantes, F. J. (1978) *J. Mol. Biol. 124*, 1–26.

Blanchard, S. G., Quast, U., Reed, K., Lee, T., & Schimerlik, M. I., Vandlen, R., Claudio, T. E., Strader, C. D., Moore, H. P. H., & Raftery, M. A. (1979) *Biochemistry 18*, 1875–1883.

Boyd, N. B., & Cohen, J. B. (1980) *Biochemistry 19*, 5344–5353.

Conti-Tronconi, B. M., & Raftery, M. A. (1982) *Annu. Rev. Biochem. 51*, 491–531.

Damle, V. N., & Karlin, A. (1978) *Biochemistry 17*, 2039–2045.

Frost, A. A., & Pearson, R. G. (1961) *Kinetics and Mechanism*, Wiley, New York.

Gage, P. W., & Hamil, O. P. (1976) *Br. J. Pharmacol. 57*, 263–272.

Heidmann, T., & Changeux, J. P. (1978) *Annu. Rev. Biochem. 47*, 317–357.

Heidmann, T., & Changeux, J. P. (1979a) *Eur. J. Biochem. 94*, 255–279.

Heidmann, T., & Changeux, J. P. (1979b) *Eur. J. Biochem. 94*, 281-296.
Janin, J. (1973) *Prog. Biophys. Mol. Biol. 27*, 77-120.
Katz, B., & Thesleff, S. (1957) *J. Physiol. (London) 138*, 63-80.
Krodel, E. K., Beckman, R. A., & Cohen, J. B. (1979) *Mol. Pharmacol. 15*, 294-312.
Lee, T., Witzemann, V., Schimerlik, M., & Raftery, M. A. (1977) *Arch. Biochem. Biophys. 183*, 57-63.
Neubig, P. R., & Cohen, J. B. (1979) *Biochemistry 18*, 5464-5474.
Neubig, P. R., & Cohen, J. B. (1980) *Biochemistry 19*, 2770-2779.
Quast, U., Schimerlik, M., Lee, T., Witzemann, T., Blanchard, S., & Raftery, M. A. (1978) *Biochemistry 17*, 2405-2414.
Quast, U., Schimerlik, M. I., & Raftery, M. A. (1979) *Biochemistry 18*, 1891-1901.
Rang, H. P., & Ritter, J. M. (1970) *Mol. Pharmacol. 6*, 357-382.
Reed, K., Vandlen, R., Duguid, J., & Raftery, M. A. (1975) *Arch. Biochem. Biophys. 167*, 138-144.
Schmidt, J., & Raftery, M. A. (1973) *Anal. Biochem. 52*, 349-354.
Sine, S., & Taylor, P. (1979) *J. Biol. Chem. 254*, 3315-3325.
Stevens, C. F. (1976) *Cold Spring Harbor Symp. Quant. Biol. 60*, 169-173.
Weber, M., David-Pfeuty, T., & Changeux, J. P. (1975) *Proc. Natl. Acad. Sci. U.S.A. 72*, 3443-3447.
Weiland, G., Georgia, B., Wee, V. T., Chignell, C. F., & Taylor, P. (1976) *Mol. Pharmacol. 12*, 1091-1105.
Weiland, G., Georgia, B., Lappi, S., Chignell, C. F., & Taylor, P. (1977) *J. Biol. Chem. 252*, 7648-7656.
Weiland, G., Frisman, D., & Taylor, P. (1979) *Mol. Pharmacol. 15*, 213-226.
Wolosin, J. M., Lydiatt, A., Dolly, J. O., & Barnard, E. A. (1980) *Eur. J. Biochem. 109*, 495-505.
Young, A. P. (1979) Ph.D. Thesis, University of California, Los Angeles, Los Angeles, CA.
Young, A. P., & Sigman, D. S. (1981) *Mol. Pharmacol. 20*, 498-505.
Young, A. P., Oshiki, J., & Sigman, D. S. (1981) *Mol. Pharmacol. 20*, 506-510.

Influence of the Peripheral Matrix Protein of Vesicular Stomatitis Virus on the Membrane Dynamics of Mixed Phospholipid Vesicles: Fluorescence Studies†

Jon R. Wiener, Ranajit Pal, Yechezkel Barenholz, and Robert R. Wagner*

ABSTRACT: In an effort to characterize the association of a peripheral membrane protein with mixed lipid bilayers, the basic ($pI \simeq 9.1$) matrix (M) protein of vesicular stomatitis virus was reconstituted with detergent-dialyzed vesicles and with preformed sonicated vesicles, each containing phospholipids with acidic head groups. The gel to liquid-crystalline phase transition of these reconstituted vesicles was studied by using steady-state fluorescence depolarization and differential polarized phase fluorometry of the hydrophobic membrane probes 1,6-diphenyl-1,3,5-hexatriene, 1-[4-(trimethylammonio)phenyl]-6-phenyl-1,3,5-hexatriene, and *trans*-parinaric acid. Reconstitution of the M protein with detergent-dialyzed vesicles composed of 50 mol % dimyristoylphosphatidylserine (DMPS) and 50 mol % dipalmitoylphosphatidylcholine (DPPC) resulted in no significant effect on the phase transition temperature as measured by all three probes. However, the M protein appeared to increase the order of the mixed lipid bilayer gel state, as evidenced by increased fluorescence anisotropy of the three probes below the transition temperature. In addition, the phase transition of the vesicle bilayer was sharpened following reconstitution with the M protein. M protein reconstituted with preformed sonicated vesicles composed of 50 mol % DPPC and 50 mol % dipalmitoylphosphatidylglycerol (DPPG) caused a large increase in the phase transition temperature as monitored by all three probes. Depending on the probe used, the observed T_m was increased from 2 to 7 °C. The M protein dramatically increased the order of the mixed lipid gel state and sharpened the lipid phase transition. Differential polarized phase fluorometry of both vesicle systems demonstrated increased order of the gel state lipid in the presence of M protein and supported the steady-state fluorescence results. These results demonstrate that binding of the peripheral membrane protein M to lipid bilayers containing acidic phospholipids results in profound alterations in the dynamics of lipid behavior in the membrane.

Vesicular stomatitis virus (VSV)[1] is a membrane-enveloped rhabdovirus which has been extensively studied as a much simpler model system than the cellular plasma membrane from which it buds (Patzer et al., 1979). The virion contains five viral-coded proteins, three of which (N, NS, and L) are associated with the single-stranded viral RNA genome to form the enzymatically active nucleocapsid core. The remaining

† From the Department of Microbiology, University of Virginia School of Medicine, Charlottesville, Virginia 22908 (J.R.W., R.P., and R.R.W.), and the Department of Biochemistry, School of Medicine, Hebrew University, Jerusalem, Israel (Y.B.). *Received October 12, 1982.* Supported by Grants MV-9E from the American Cancer Society, PCM77-00494 from the National Science Foundation, AI-11112 and HL-17576 from the National Institutes of Health, and 2669 from the U.S.A.-Israel Binational Science Foundation. J.R.W. is a Predoctoral Trainee of Grant CA-09109 from the National Cancer Institute.

[1] Abbreviations: DPPC, dipalmitoylphosphatidylcholine; DMPS, dimyristoylphosphatidylserine; DPPG, dipalmitoylphosphatidylglycerol; VSV, vesicular stomatitis virus; M, VSV matrix protein; DPH, 1,6-diphenyl-1,3,5-hexatriene; TMA-DPH, 1-[4-(trimethylammonio)-phenyl]-6-phenyl-1,3,5-hexatriene; TPA, *trans*-parinaric acid; T_m, lipid phase transition midpoint temperature; Tricine, *N*-[tris(hydroxymethyl)methyl]glycine.

0006-2960/83/0422-2162$01.50/0